

# The Timing of Nine Globular Cluster Pulsars

Ryan S. Lynch<sup>1,2</sup>, Paulo C. C. Freire<sup>3</sup>, Scott M. Ransom<sup>4</sup>, and Bryan A. Jacoby<sup>5</sup>

## ABSTRACT

We have used the Robert C. Byrd Green Bank Telescope to time nine previously known pulsars without published timing solutions in the globular clusters M62, NGC 6544, and NGC 6624. We have full timing solutions that measure the spin, astrometric, and (where applicable) binary parameters for six of these pulsars. The remaining three pulsars (reported here for the first time) were not detected enough to establish solutions. We also report our timing solutions for five pulsars with previously published solutions, and find good agreement with past authors, except for PSR J1701–3006B in M62. Gas in this system is probably responsible for the discrepancy in orbital parameters, and we have been able to measure a change in the orbital period over the course of our observations. Among the pulsars with new solutions we find several binary pulsars with very low mass companions (members of the so-called “black widow” class) and we are able to place constraints on the mass-to-light ratio in two clusters. We confirm that one of the pulsars in NGC 6624 is indeed a member of the rare class of non-recycled pulsars found in globular clusters. We also have measured the orbital precession and Shapiro delay for a relativistic binary in NGC 6544. If we assume that the orbital precession can be described entirely by general relativity, which is likely, we are able to measure the total system mass ( $2.57190(73) M_{\odot}$ ) and companion mass ( $1.2064(20) M_{\odot}$ ), from which we derive the orbital inclination ( $\sin i = 0.9956(14)$ ) and the pulsar mass ( $1.3655(21) M_{\odot}$ ), the most precise such measurement ever obtained for a millisecond pulsar. The companion is the most massive known around a fully recycled pulsar.

---

<sup>1</sup>Physics Department, McGill University, 3600 Rue University, Montréal, QC, Canada H3A 2T8, [rylynch@physics.mcgill.ca](mailto:rylynch@physics.mcgill.ca)

<sup>2</sup>Department of Astronomy, University of Virginia, P.O. Box 400325, Charlottesville, VA 22904-4325

<sup>3</sup>Max-Planck-Institut für Radioastronomie, Auf dem Hügel 69, D-53121 Bonn, Germany, [pfreire@mpifr-bonn.mpg.de](mailto:pfreire@mpifr-bonn.mpg.de)

<sup>4</sup>National Radio Astronomy Observatory, 520 Edgemont Road, Charlottesville, VA 22903-4325, [sransom@nrao.edu](mailto:sransom@nrao.edu)

<sup>5</sup>Affiliated with The Aerospace Corporation, 15049 Conference Center Drive, Chantilly, VA 20151-3824, [bryan.jacoby@gmail.com](mailto:bryan.jacoby@gmail.com)

*Subject headings:* globular clusters: individual (M62, NGC 6544, NGC 6624)—  
pulsars: individual (J1701–3006D, J1701–3006E, J1701–3006F, J1807–2459A,  
J187–2500B, J1823–3021C, J1823–3021D, J1823–3021E, J1823–3021F)

## 1. Introduction

Millisecond pulsars (MSPs) form by “recycling” a dormant neutron star through the accretion of mass and angular momentum from a binary companion (Alpar et al. 1982). This leads to a very rapidly rotating and stable pulsar with a relatively low magnetic field ( $\sim 10^9$  G) and long lifetime ( $\gtrsim 10^9$  yr). MSPs form naturally in the dense environments of globular clusters (GCs), thanks to frequent exchange interactions that may lead to the formation of mass transferring binaries (Camilo & Rasio 2005). Sensitive searches of GCs have uncovered 144 pulsars in 28 clusters<sup>6</sup>, and the vast majority of these are recycled MSPs. Indeed, nearly half of all MSPs have been discovered in GCs<sup>7</sup>.

The same interactions that form MSPs so efficiently in clusters also lead to many exotic systems that are rarely seen in the disk of the Galaxy. These include the fastest spinning MSP (Hessels et al. 2006), highly eccentric binaries (Ransom et al. 2005; Freire et al. 2007), massive neutron stars (Freire et al. 2008), pulsar-main sequence binaries (D’Amico et al. 2001b), and many “black widow” systems (King et al. 2005). These discoveries demonstrate the huge scientific payoff that can come from the discovery of unique pulsars thanks to two factors—the extreme nature of neutron stars, which opens windows on otherwise inaccessible realms of physics, and the extraordinary clock-like nature of MSPs. The bedrock of pulsar astronomy is *timing*, the process of creating a model that unambiguously accounts for every rotation of the pulsar, thus probing the pulsar and its environment. For MSPs, the arrival time of a pulse can typically be measured to within a few microseconds or better (e.g. Verbiest et al. 2008), which enables very precise timing models. Timing GC pulsars leads to unique challenges, though. Because GCs are usually at a distance of several kiloparsecs, the flux density of their constituent MSPs is usually very low, necessitating very long integration times. Another consequence of cluster distances is very high dispersion measures, which necessitate moving to higher observing frequencies (e.g. 2 GHz) where pulsars tend to be weaker. Luckily, since many clusters contain several MSPs that can each be observed during a single observation, the required observing time is well spent.

---

<sup>6</sup>See <http://www.naic.edu/~pfreire/GCpsr.html> for an up-to-date list.

<sup>7</sup>There are 160 field pulsars with period  $P < 20$  ms in the ATNF catalog, and 131 GC pulsars that meet the same criteria (see <http://www.atnf.csiro.au/people/pulsar/psrcat/>).

In addition to recycled MSPs, a small population of slow, non-recycled pulsars have also been observed in a handful of clusters (Lyne et al. 1996; Boyles et al. 2011). Their presence is something of a mystery, because they resemble in every way the “normal” pulsars that are so numerous in the Galactic disk, but which have lifetimes  $\sim 10^7$ – $10^8$  yr and are thought to form through core collapse supernovae of massive stars. However, GCs are old stellar systems with typical ages  $10^{10}$  yr (Carretta et al. 2000), so all stars massive enough to form pulsars should have died some  $10^{10}$  yr ago. As such, the core collapse of massive stars cannot be the avenue through which non-recycled pulsars in GCs have formed. The most popular alternative formation scenario involves the collapse of a massive white dwarf via electron capture (Nomoto 1984, 1987), though the details of these so-called electron capture supernovae are not well understood.

In this paper, we present new timing solutions for nine pulsars spread across three GCs—M62, NGC 6544, and NGC 6624. Each of these clusters contains multiple MSPs and NGC 6624 contains two non-recycled pulsars. All of these pulsars were discovered elsewhere, but full, phase-connected timing solutions have only been published for five of them (see Table 1 for a summary and list of references). We also present our solutions for these five. We began a timing campaign using the Robert C. Byrd Green Bank Telescope (GBT) for the nine pulsars without full solutions, starting in 2009 February. We have managed to obtain full solutions that include measurement of the first period derivative for six of these pulsars. A combination of low flux densities and an irreversible data processing error conspired to prevent us from obtaining full solutions for the two remaining MSPs, but we are in a position to comment on them in further detail. Our most exciting result is the discovery of a massive companion orbiting a fully recycled MSP. In §2 we describe our observations and in §3 outline our method for timing the pulsars and further data analysis. A discussion of individual systems can be found in §4, and we provide a summary in §5.

## 2. Observing Scheme

Observations were carried out with the GBT, observing at a frequency of 2.0 GHz using 800 MHz of bandwidth, although persistent radio frequency interference (RFI) reduced the usable bandwidth to  $\sim 600$  MHz. This frequency was chosen to overcome the deleterious effects of dispersive smearing caused by free electrons in the ISM, and has been used successfully by our group before. Data were recorded in the PSRFITS<sup>8</sup> (Hotan et al. 2004) format using the Green Bank Ultimate Pulsar Processor (GUPPI) (DuPlain et al. 2008) with a  $64 \mu\text{s}$

---

<sup>8</sup><http://www.atnf.csiro.au/research/pulsar/psrfits/index.html>

sampling time and 2048 frequency channels across the entire bandwidth. We typically observed NGC 6544 for 30 minutes, and M62 and NGC 6624 for 45–60 minutes each, although the exact integration times varied between observations. In general, data were relatively free of RFI, but when necessary, we used the RFI excision tools in the PRESTO<sup>9</sup> software suite to mask out contaminated portions of the data.

We also used archival GBT data taken in 2004. These data were collected using the GBT Pulsar Spigot (Kaplan et al. 2005) at either 820 MHz (with 50 MHz of bandwidth) or at 2 GHz (with the same bandwidth as above). Most of these observations used 2048 frequency channels and 40.96  $\mu$ s sampling, although some used 1024 channels and 81.92  $\mu$ s sampling. All of these data were analyzed using PRESTO.

The pulsars in NGC 6544 were observed again in 2011 as part of a campaign to measure Shapiro delay in PSR J1807–2500B (see 4.6). These data were collected using GUPPI in a coherent de-dispersion search mode (i.e. a filterbank where each channel was coherently de-dispersed) at 1.4 GHz using 800 MHz of bandwidth. For these observations we used 512 frequency channels and 10.24  $\mu$ s sampling.

### 3. Timing and Data Analysis

Data were processed using a combination of PRESTO and PSRCHIVE<sup>10</sup>. All of the folded pulse profiles were phase-aligned and summed to create high signal-to-noise (S/N) profiles. The profiles were fit with one or more Gaussians, from which standard pulse templates were made and used to obtain pulse times of arrival (TOAs) via cross-correlation in the Fourier domain. We typically obtained three to six TOAs per pulsar per observation depending on the S/N of that observation, though some pulsars (such as NGC 6544A) were sufficiently bright that many precise TOAs could be measured. Timing solutions were constructed by performing a weighted fit to the data using TEMPO2<sup>11</sup> (Edwards et al. 2006) with the DE405 Solar System ephemeris and TT(BIPM2011) time standard. All values are reported in Barycentric Dynamical Time. It is not uncommon for timing models to have a reduced  $\chi^2 > 1$  ( $\chi_{\text{red}}^2$ ) even after all parameters have been well measured. When no systematic trends are present in the data, it is assumed that this value of  $\chi_{\text{red}}^2$  is due to an underestimate of the error on individual TOAs. As is common practice, we deal with this situation by multiplying

---

<sup>9</sup><http://www.cv.nrao.edu/~sransom/presto/>

<sup>10</sup><http://psrchive.sourceforge.net/>

<sup>11</sup><http://sourceforge.net/projects/tempo2/>

TOA errors by a small constant error factor so that  $\chi_{\text{red}}^2 = 1$ .

### 3.1. Corrections for Cluster Acceleration

MSPs have a small intrinsic rate of spin-down ( $\dot{P}_{\text{int}}$ ) that is usually heavily contaminated by accelerations within the potential of the cluster and Galaxy (Phinney 1993). This makes it impossible to measure their spin-down related properties (surface magnetic field, spin-down luminosity, and characteristic age) directly. Instead, we calculate the limit

$$\frac{\dot{P}_{\text{int}}}{P} \leq \frac{\dot{P}_{\text{obs}}}{P} + \frac{a_{\text{c,max}}}{c} + \frac{a_{\text{G}}}{c} + \frac{\mu^2 D}{c} \quad (1)$$

where  $P$  is the pulsar period,  $a_{\text{c,max}}$  and  $a_{\text{G}}$  are the accelerations due to the cluster and Galaxy, respectively,  $\mu$  is the proper motion,  $D$  is the distance to the cluster, and  $c$  is the speed of light (the last term accounts for the Shklovskii effect (Shklovskii 1970)). Phinney (1992, 1993) showed that to within 10% accuracy,

$$\frac{a_{\text{c,max}}}{c} \approx \frac{3\sigma_v^2}{2c(R_c^2 + R_{\text{psr}}^2)^{1/2}} \quad (2)$$

for  $R_{\text{psr}} < 2R_c$ , where  $\sigma_v$  is the central velocity dispersion,  $R_c$  is the core radius, and  $R_{\text{psr}}$  is the projected distance of the pulsar from the center of the cluster. Because all three of the clusters studied here are core collapsed, analytical (Freire et al. 2005) and numerical models are not applicable, which is why we use the approximations of Phinney. These were developed for use with pulsars in M15, which is also core collapsed. We use the values of  $R_c$  found in Harris (1996, 2010 edition). The following references are used for  $\sigma_v$ : Harris (1996, 2010 edition) for M62; Webbink (1985) for NGC 6544; and Valenti et al. (2011) for NGC 6624. Table 2 lists the relevant properties of each cluster. The Galactic contribution is calculated under the approximation of a spherically symmetric Galaxy with a flat rotation curve (Phinney 1993) and is

$$\dot{P}_{\text{Gal}} = -7 \times 10^{-19} \left( \frac{P}{\text{s}} \right) \left( \cos b \cos \ell + \frac{\delta - \cos b \cos \ell}{1 + \delta^2 - 2\delta \cos b \cos \ell} \right) \quad (3)$$

where  $b$  and  $\ell$  are the Galactic latitude and longitude of the cluster,  $\delta = R_0/D$  and  $R_0$  is the Sun's Galactocentric distance. However, the cluster term is usually dominant.

### 3.2. Flux Calibration and Rotation Measure

Rough mean flux density ( $S_\nu$ ) estimates were made by assuming that the off-pulse RMS noise level was described by the radiometer equation,

$$\sigma = \frac{T_{\text{tot}}}{G\sqrt{n_{\text{pol}}\Delta\nu t_{\text{obs}}}} \quad (4)$$

where  $T_{\text{tot}}$  is the total system temperature,  $G$  is the telescope gain,  $n_{\text{pol}} = 2$  is the number of summed polarizations, and  $\Delta\nu$  is the bandwidth. For the GBT 2 GHz receiver,  $G = 1.9 \text{ K Jy}^{-1}$  and  $T_{\text{sys}} \approx 23 \text{ K} + T_{\text{sky}}$ , where  $T_{\text{sky}}$  is the contribution from the Galactic synchrotron emission. This was calculated by scaling the values from Haslam et al. (1982) with a spectral index of  $-2.6$ . The typical uncertainty in these estimates of  $S_\nu$  is 10%–20%. We were able to record full polarization data for one observation per cluster. These were calibrated using the 25 Hz noise diode on the GBT, and we searched for a significant rotation measure (RM) by looking for a peak in the polarized flux. We searched from  $-1000$  to  $1000 \text{ rad m}^{-2}$ , but in most cases, the S/N was not sufficient to constrain RM. The notable exceptions are the two pulsars in NGC 6544, for which we measure an average RM of  $\sim 158 \text{ rad m}^{-2}$ . Figure 1 shows the fully calibrated, RM corrected profiles of NGC 6544A and B.

## 4. Discussion of Individual Systems

All of our timing solutions can be found in Tables 3–7, along with some derived properties of the pulsars. Average pulse profiles and Doppler modulated pulse periods of the binary pulsars in these clusters are shown in Figs. 2 & 3. Post-fit timing residuals are shown in Fig. 4. We discuss each individual system below.

### 4.1. Pulsars with Previously Published Timing Solutions

PSRs J1701–3006A, B, and C and J1823–3021A and B all have timing solutions published by other authors (Possenti et al. 2003; Biggs et al. 1994). We constructed our own timing solutions based solely on our data to confirm that there were no irregularities in our data or methods. We find that nearly all our measured parameters agree with those published elsewhere to within errors<sup>12</sup>. The one major exception to this is PSR J1701–3006B

---

<sup>12</sup>Our measurement of right ascension for M62A differs from the results given in Possenti et al. (2003) by  $0.003''$ , which is approximately five times the formal  $1\text{-}\sigma$  errors

(hereafter M62B), where we see a highly significant change in orbital period and dispersion measure (DM) compared with the results of Possenti et al. (2003). We have also measured the rate of change of the orbital period  $\dot{P}_b = -5.51(62) \times 10^{-12}$ . We performed an F-test to determine if the addition of  $\dot{P}_b$  was indeed required by the data. Without it,  $\chi^2 = 142.82$  with 71 degrees of freedom, while after fitting for  $\dot{P}_b$  the  $\chi^2$  improved to 73.94 with 70 degrees of freedom. The probability that this improvement is due to chance is  $< 1.3 \times 10^{-11}$ , so the measured  $\dot{P}_b$  does indeed seem to be required by the data. M62B is known to eclipse and has an optical and X-ray counterpart (Cocozza et al. 2008). As Cocozza et al. discuss, the pulsar and companion star are almost certainly interacting. The contribution to  $\dot{P}_b$  expected from general relativity (GR) is two orders of magnitude smaller than observed, assuming  $M_p = 1.4 M_\odot$  and  $M_c = M_{c,\min}$ , and there is no realistic combination of pulsar and companion masses and inclination angles that would lead to such a large relativistic  $\dot{P}_b$ . As such, classic tidal effects of the extended companion are probably the cause of the change in orbital period. Our RMS timing residuals are over a factor of two smaller than obtained by Possenti et al. (2003), which probably explains why we were able to detect  $\dot{P}_b$  even though we had a shorter timing baseline.

#### 4.2. PSR J1701–3006D

PSR J1701–3006D (hereafter M62D) is a 3.42 ms binary MSP. M62D (along with E and F) were discovered, and initial orbital solutions were given, by Chandler (2003). The orbital period is 1.1 days, with a small eccentricity<sup>13</sup>,  $e \sim 4.12 \times 10^{-4}$ . The minimum companion mass is  $\sim 0.12 M_\odot$  (assuming a  $1.4 M_\odot$  MSP), and is likely a white dwarf. We see no evidence for eclipses in M62D, but none of our observations cover conjunction, when an eclipse would be most likely. Three observations do, however, start or end within four hours ( $\sim 15\%$  of the orbital period) of conjunction, and one observation ends only 15 minutes before conjunction. The lack of eclipses increase our confidence that the companion is a white dwarf, and not a main sequence (MS) star (for which eclipses should be common). We are unable to measure any precession in the longitude of periastron, so no further constraints can be placed on the mass or geometry of the system at this time. The acceleration of M62D ( $\dot{P}P^{-1}$ ) is somewhat higher than for the majority of GC pulsars (Ransom 2008), though not exceedingly so. We note, though, that PSRs J1701–3006E and F have similarly large accelerations.

---

<sup>13</sup>We have used the ELL1 timing model in TEMP02, which is appropriate when  $a \sin i / c e^2 \ll 1$  (Lange et al. 2001).

### 4.3. PSR J1701–3006E

PSR J1701–3006E (hereafter M62E) is a 3.23 ms binary MSP in a circular orbit. The orbital period is only 3.80 hr, and the projected semi-major axis is only  $0.0302 R_{\odot}$ . When combined with the low minimum companion mass ( $0.031 M_{\odot}$ , or only 31 Jupiter masses) and the presence of eclipses, M62E is clearly a black widow pulsar (King et al. 2005). The presence of eclipses makes it likely that the system is being seen at a high inclination, so that the true companion mass is probably close to the minimum. We have good orbital coverage of the system, and observe both ingress and egress during eclipses, which are sharp and do not lead to a significant change in DM. The eclipses are centered around orbital conjunction and occur for  $\sim 12\%$  of the orbit (or roughly 12 minutes). We see no evidence for eclipses at other orbital phases. The projected extent of the eclipsing material is  $\sim 7 \times 10^5$  km. A relationship for the radius of the companion is given by King (1988):

$$R_c \simeq 10^4 \text{ km} (1 + X)^{5/3} \left( \frac{M_c}{M_{\odot}} \right)^{-1/3} \quad (5)$$

where  $X$  is the hydrogen fraction. For  $X = 0.7$  we find  $R_c \sim 8 \times 10^4$  km, which is substantially smaller than the implied size of the eclipsing region. It seems likely that the eclipses are being caused by an extended region of gas surrounding the companion.

### 4.4. PSR J1701–3006F

PSR J1701–3006F (hereafter M62F) is a 2.29 ms binary MSP in a circular orbit. Like M62E, it has a low minimum mass companion ( $\sim 22$  Jupiter masses) and occupies a region in  $M_{c,\min}$ - $P_b$  phase space typical of non-eclipsing black widow pulsars. Indeed, despite full orbital coverage we see no evidence for flux variability as a function of orbital phase. Nonetheless, given the very low mass limit and highly circularized orbit, we still favor classifying M62F as a black widow, and the lack of eclipses probably indicate that the system is not being viewed close to edge-on (Freire 2005).

### 4.5. PSR J1807–2459A

PSR J1807–2459A (NGC 6544A) has already been discussed extensively by D’Amico et al. (2001a) and Ransom et al. (2001). It is a 3.06 ms MSP in a black widow system with a highly circular orbit and  $M_{c,\min} = 0.009 M_{\odot}$ . We were able to reliably phase connect the data collected in 2009–2010 to data taken in 2011 as part of our Shapiro delay observations of PSR



J1807–2500B (see below), as well as to older GBT data from 2004<sup>14</sup>. The orbital parameters of this system were already well determined by previous authors, however no phase-coherent timing solution had ever been derived or published. Our new timing solution includes, for the first time, a precise measurement of the position of the system and its spin-down. The orbit in our solution is in good agreement with previous analyses, but significantly more precise; it allowed us to measure  $\dot{P}_b$ . Like M62B, the GR contribution to  $\dot{P}_b$  is two orders of magnitude smaller than observed for a 1.4  $M_\odot$  pulsar and minimum mass companion. However, there are no eclipses observed for NGC 6544A, so it is possible that the orbital inclination is significantly smaller than  $90^\circ$ , which would imply a higher companion mass and larger GR contribution. Nonetheless, for GR to contribute even 10% of the measured  $\dot{P}_b$ , the companion would have to have a mass of  $\sim 0.06 M_\odot$ , corresponding to  $i = 9^\circ$ . For a distribution of inclination angles that is flat in  $\cos i$ , there is only a  $\sim 1\%$  probability of having  $i < 9^\circ$ . It thus seems that we can safely rule out a significant contribution from GR to  $\dot{P}_b$ . We can also rule out significant contamination from acceleration in the cluster because the observed  $\dot{P}_b/P_b$  is several times larger than the maximum cluster acceleration. It thus seems likely that  $\dot{P}_b$  can be explained by normal long-term black widow behavior (Nice et al. 2000). NGC 6544A is offset from the center of the cluster by  $4.6''$ , or roughly 1.5 core radii. At the distance of NGC 6544, this is only 0.06 pc.

The observed  $\dot{P} < 0$ , which, if it were intrinsic to the pulsar, would imply that the pulsar is spinning *up*. In reality,  $\dot{P}$  is contaminated by the acceleration of the pulsar within the gravitational field of the cluster and Galaxy, and the fact that  $\dot{P} < 0$  gives unambiguous evidence that the pulsar is on the far side of the cluster and accelerating towards Earth. This provides us with a probe of the mass enclosed at the projected position of the pulsar and the mass-to-light ratio ( $\Upsilon$ ) (Phinney 1993). Following D’Amico et al. (2002),

$$\Upsilon_V \geq 1.96 \times 10^{17} \frac{a_c}{c} \left( \frac{\Sigma_V(< \theta_\perp)}{10^4 L_{\odot,V} \text{ pc}^{-2}} \right)^{-1} \quad (6)$$

where  $\Sigma_V(< \theta_\perp)$  is the mean surface brightness interior the position of the pulsar. To calculate  $\Sigma_V(< \theta_\perp)$ , we assume a constant surface brightness in the core of the cluster. The cluster acceleration,  $a_c$ , is obtained by re-arranging Eq. 1. In this case, the intrinsic spin-down of the pulsar is estimated by using the formula for characteristic age ( $\tau_c$ ),

$$\frac{\dot{P}_{\text{int}}}{P} \approx \frac{1}{2\tau_c}, \quad (7)$$

---

<sup>14</sup>The difference between the pre-fit residuals of the 2004 data and the predictions of our 2009–2011 based timing solution are only 6% of pulse phase. Therefore, we are confident that we can phase connect all our data.

assuming a pulsar age of 10 Gyr. We find  $\dot{P}_{\text{int}}/P = 1.6 \times 10^{-18} \text{ s}^{-1}$ . We were unable to find a proper motion for NGC 6544 in the literature, but our results are not very sensitive to this—for example, if the cluster had a transverse velocity of  $100 \text{ km s}^{-1}$ , it would affect our results at the 10% level. Combining all of this information, we find  $\Upsilon_V \geq 0.072 M_\odot/L_\odot$ . Massive stellar remnants in the cores of GCs should give rise to a higher  $\Upsilon_V$  (typically  $\sim 3\text{--}4 M_\odot/L_\odot$ ), so this result is very unconstraining.

#### 4.6. PSR J1807–2500B

PSR J1807–2500B (NGC 6544B; Chandler 2003) is the most intriguing system in our sample. As with NGC 6544A, we were able to phase connect data spanning 2004–2011<sup>15</sup>. The pulsar has a period of 4.19 ms and is in a highly eccentric orbit, with  $e = 0.747$  (see Fig. 3). The very high eccentricity of this system has allowed us to measure a very significant precession of periastron,  $\dot{\omega} = 0.018319(12)^\circ \text{ yr}^{-1}$ . We have also measured Shapiro delay in NGC 6544B<sup>16</sup>. We discuss both measurements in more detail below.

##### 4.6.1. Possible Contributions to $\dot{\omega}$

The observed orbital precession could be due to any combination of tidal deformation of the companion, spin-orbit coupling, or GR effects, but for various reasons discussed below, we believe that it is due almost entirely to GR.

Tidal deformation of the companion would require a MS or giant companion. This already seems unlikely based solely on the mass function—the minimum companion mass for  $M_p = 1.4 M_\odot$  is  $\sim 1.2 M_\odot$ , which is well above the turn-off mass in GCs ( $\sim 0.8 M_\odot$ ). Even if we use a smaller pulsar mass (say  $1.2 M_\odot$ ), the minimum companion mass is still  $\sim 1.1 M_\odot$ . This rules out a MS companion, unless it was a blue straggler, but given how rare these are, this seems exceedingly unlikely. Any giants would have to be close to the turn-off mass and would experience Roche lobe overflow. The resulting gas in the system would give rise to eclipses, especially if the orbit is highly inclined (and as we show below, it is) and near conjunction. As it turns out, we see no evidence for eclipses at any orbital phase, including conjunction, so a giant seems unlikely. A blue straggler would also probably cause eclipses

---

<sup>15</sup>The difference between the pre-fit residuals of the 2004 data and the predictions of our 2009–2011 based timing solution are  $< 3\%$  of pulse phase. Therefore, we are confident that we can phase connect all our data.

<sup>16</sup>To the best of our knowledge, this is the first detection of Shapiro delay in a GC pulsar.

or some other timing irregularities in the pulsar. In fact, NGC 6544B times remarkably well, with no unmodeled trends in the data and no need for an error factor to bring  $\chi_{\text{red}}^2 = 1$ . Hence, we can safely rule out a significant contribution to  $\dot{\omega}$  by tidal deformation.

Spin orbit coupling is a possibility if the companion is rapidly rotating, but it scales as  $|\dot{x}/x|$  times a geometrical factor, where  $x$  is the projected semi-major axis; the geometrical factor is expected to be  $< 10$  in 80% of cases (e.g. Freire et al. 2008, and references therein). Our current best limit on  $\dot{x}$  implies that precession due to spin-orbit coupling should be smaller than our extremely small measurement uncertainties in  $\dot{\omega}$

For the reasons outlined above, we feel confident that the observed  $\dot{\omega}$  is due almost entirely to GR. In this case the total mass of the system is given by

$$\frac{M_{\text{tot}}}{M_{\odot}} = \left(\frac{\dot{\omega}}{3}\right)^{3/2} \frac{(1 - e^2)^{3/2}}{T_{\odot}} \left(\frac{P_{\text{b}}}{2\pi}\right)^{5/2}, \quad (8)$$

where  $T_{\odot} = GM_{\odot}c^{-3}$ , and  $P_{\text{b}}$  is the orbital period. Using our measured values, we find  $M_{\text{tot}} = 2.56763(59) M_{\odot}$ .

#### 4.6.2. Shapiro Delay Measurement

The total system mass of NGC 6544B is fairly high for a pulsar binary system. When combined with the observed mass function, it implies a high orbital inclination and massive companion, making NGC 6544B an excellent candidate for a measurement of Shapiro delay. We observed the pulsar on ten occasions over a variety of orbital phases, including two eight hour tracks at or near orbital conjunction<sup>17</sup>.

We used the DDH timing model developed by Freire & Wex (2010), which parameterizes the Shapiro delay as

$$\varsigma \equiv \frac{s}{1 + \sqrt{1 - s^2}} \quad (9)$$

$$h_3 \equiv r\varsigma^3 \quad (10)$$

where  $s = \sin i$  and  $r = T_{\odot}M_c$  are the traditional Shapiro delay parameters. In this parameterization,  $h_3$  quantifies the amplitude of the third harmonic and  $\varsigma$  the ratio of successive

---

<sup>17</sup>Because the orbital period is almost exactly ten days, conjunction moves slowly in sidereal time, and as such is not visible from a given telescope for long stretches. We were not able to schedule all our observations contiguously around conjunction due to this constraint.

harmonics of the Shapiro delay. These parameters are less correlated with each other and with other orbital parameters than are  $s$  and  $r$ , and provide a better description of the combinations of orbital inclination and companion mass allowed by the timing. From the measured values of  $h_3$  and  $\varsigma$  we derive  $\sin i = 0.99715(20)$  and  $M_c = 1.02(17) M_\odot$ . On its own, the Shapiro delay does not provide precise measurements of the component masses, but the DDH model does not assume that  $\dot{\omega}$  is relativistic, and thus does not make full use of the available information.

To improve our mass estimates we used the DDGR model (Taylor & Weisberg 1989), which assumes that GR correctly describes the system. In this model,  $M_{\text{tot}}$  and  $M_c$  are free parameters and all post-Keplerian (PK) parameters are derived from these measurements. From this we obtain  $M_{\text{tot}}^{\text{DDGR}} = 2.57190(73) M_\odot$ ,  $M_c^{\text{DDGR}} = 1.2064(20) M_\odot$ , and derive  $M_p^{\text{DDGR}} = 1.3655(21) M_\odot$  (see Table 6 for the complete solution). This is the most precise mass ever derived for an MSP, the previous being J1903+0327 (Freire et al. 2011). To understand this exceptional precision and verify it, we created  $\chi^2$  maps from the DDH model, using the Keplerian parameters of the DDGR solution as a starting point. For each  $\cos i$  and  $M_c$ , we calculated all five PK parameters ( $\dot{\omega}$ ,  $\gamma$ ,  $\dot{P}_b$ ,  $\varsigma$  and  $h_3$ ) assuming they are determined solely by GR; these were kept fixed while TEMPO2 fit for all other parameters. The resulting  $\chi^2$  values were recoded and the associated 2-D probability distribution function (PDF) was calculated using the Bayesian analysis technique discussed in detail in Splaver et al. (2002). This 2-D PDF was then translated into the  $M_c$ - $M_p$  plane using the mass function of our starting DDH solution. The original 2-D PDF was then collapsed onto the  $\cos i$  and  $M_c$  axes, with the derived 2-D PDF collapsed into the  $M_p$  axis (see red lines in Fig. 5), generating 1-D PDFs for the latter quantities. These are slightly asymmetric; they have medians and  $\pm 1\sigma$  percentiles at:  $\cos i^{\text{med}} = 0.097_{-0.015}^{+0.017}$ ,  $M_p^{\text{med}} = 1.3649_{-0.0022}^{+0.0017} M_\odot$ , and  $M_c^{\text{med}} = 1.2068_{-0.0016}^{+0.0022} M_\odot$ . The maximum probability occurs at  $\cos i^{\text{max}} = 0.095$ ,  $M_p^{\text{max}} = 1.3654 M_\odot$ , and  $M_c^{\text{max}} = 1.2063 M_\odot$ . These are in excellent agreement with the best-fit results of the DDGR model, and confirm the value and the small uncertainty of the masses.

The regions of the  $\cos i$ - $M_p$  plane (and derived  $M_p$ - $M_c$  plane) allowed by each measured PK parameter are depicted in Fig. 5. This allows us to understand the reason for such a precise mass: the constraint provided by  $\dot{\omega}$  (the total mass  $M_{\text{tot}}$ , according to GR) cuts the  $\cos i$ - $M_c$  (or  $M_p$ - $M_c$ ) regions allowed by the Shapiro delay very sharply.

The measured companion mass strengthens the case made in §4.6.1 that the companion must be a massive white dwarf or second neutron star. The companion is the most massive known around a fully recycled pulsar. If this is a double neutron star system, it is only the second known in GCs, the first being M15C (Anderson et al. 1990; Jacoby et al. 2006). It is likely that the pulsar was recycled by a different companion, which was then ejected in

an exchange interaction. Deep Hubble Space Telescope images of the cluster may be able to detect a white dwarf companion, while a non-detection of the companion would strengthen the case for a double neutron star system.

We have measured three PK parameters ( $\dot{\omega}$ ,  $\zeta$ , and  $h_3$ ). Assuming GR is correct, all three agree on the same region of the  $M_c$ - $M_p$  plane. As such, GR passes this test, albeit at relatively low precision. Our current best measurement of a fourth PK parameter, the gravitational redshift, is  $\gamma = 0.026(14)$  s. This is consistent with the GR prediction of 0.014 s. We plan to continue monitoring this system long-term, and in a few years expect to have a more precise measurement of  $\gamma$  that will allow for a second test of GR.

#### 4.7. PSR J1823–3021C

PSR J1823–3021C (NGC 6624C) has  $P = 0.406$  s, unusually slow among globular cluster pulsars but, surprisingly, the second such slow pulsar in NGC 6624. It was discovered by Chandler (2003); we have now measured, for the first time,  $\dot{P} = 2.25 \times 10^{-16}$  s s $^{-1}$ . Using Eq. 2, we find  $\dot{P}_{c,\max} = 1.7 \times 10^{-17}$  s s $^{-1}$ , over an order of magnitude smaller than the measured  $\dot{P}$ . The contributions from the Galaxy and the Shklovskii effect are even smaller still, so it is clear that the observed  $\dot{P}$  is due almost entirely to the intrinsic pulsar spin-down. The implied characteristic age and surface magnetic field is  $\tau_c \sim 2.8 \times 10^7$  yr and  $3.1 \times 10^{11}$  G. This makes NGC 6624C, like NGC 6624B, similar to the “normal”, non-recycled pulsars (NRPs) usually seen in the Galactic disk. As explained in §1, NRPs are typically assumed to form in core collapse supernova, which require massive stars that have not existed in GCs for billions of years. Since NRPs have lifetimes  $\ll 10^9$  yr, core collapse supernovae cannot explain the presence of NGC 6624C and pulsars like it. The leading alternative explanation is electron capture supernovae (ECS). The kick velocities ( $v_{\text{kick}}$ ) that pulsars receive when they form via ECS are not well known, though there is evidence that  $v_{\text{kick}} \sim 10$  km s $^{-1}$  (Pfahl et al. 2002; Kitaura et al. 2006; Dessart et al. 2006; Martin et al. 2009; Wong et al. 2010). The escape velocity from the center of NGC 6624 is  $\sim 35$  km s, which effectively places an upper bound on the  $v_{\text{kick}}$  that NGC 6624C received. This supports the notion that ECS kicks are much smaller than those induced by core collapse supernovae.

GC NRPs can also enable useful statistical constraints on the properties of ECS (Boyles et al. 2011; Lynch et al. in prep.). NGC 6624C is one of only four GC NRPs known, making it an important addition to this rare family of pulsars.

#### 4.8. Pulsars Without Full Timing Solutions

As part of this work, we discovered three previously unknown MSPs, J1823-3021D, E, and F (hereafter NGC 6624D, E, and F). However, we were unable to obtain full timing solutions for them. This was due to the very low signal-to-noise ratio of the detections of all three pulsars, due in part to their low flux densities, but also due to a data processing error on our part. As is typical, we de-dispersed the raw data and combined many frequency channels to reduce data volume (i.e. sub-banding), discarding the raw data afterward. However, we accidentally de-dispersed at the wrong DM for many of our observations, thereby adding significant dispersive smearing and degrading the signal from these already weak pulsars even further. Without the raw data, we are unable to remedy this error. PSR J1823–3021A was bright enough that it could still be detected, and the dispersive smearing was not large enough to significantly impact the two long-period pulsars. Despite this, we could still determine some of the basic properties of NGC 6624D, E, and F.

We are able to confirm that NGC 6624D and E are isolated MSPs with  $P = 3.02$ , and  $4.39$  ms, respectively. NGC 6624D was detected on many occasions, but the TOA errors were quite large. We were able to measure the position with some accuracy, although without a reliable measurement of  $\dot{P}$ , we are unable to break all the covariances in the fit, so these coordinates should be used cautiously. NGC 6624E was only detected in three observations but there was no variation in the apparent period of the pulsar between these observations, nor was there any evidence of acceleration. Both of these effects are expected if the pulsar were in a binary system. We were unable to phase connect any of our observations due to large relative errors on the measured period of the pulsar, and we cannot constrain its position or  $\dot{P}$ .

NGC 6624F is an eclipsing binary MSP with  $P = 4.85$  ms. Like NGC 6624E, NGC 6624F was only detected three times. In each case, we were able to clearly measure variations in  $P$ ,  $\dot{P}$  and  $\ddot{P}$  arising from orbital motion. As it turns out, the apparent period of the pulsar was similar and the acceleration was positive in all three observations, indicating that the observations occurred at overlapping orbital phases near inferior conjunction. Because the pulsar had the *exact* same apparent period at some point during each of our observations, there must have been an integer number of orbits between these times. We calculated the exact moment during each observation when the pulsar had a reference barycentric period of precisely 4.85 ms through a Taylor expansion of  $P$ ,  $\dot{P}$ , and  $\ddot{P}$  and a bisection method. An orbital period of 0.8827 days implies exactly 106.0003 and 146.9996 complete orbits between our three observations. The fact that we were able to fit such a precise integer number of orbits gives us confidence that this is the true orbital period of the system. If NGC 6624F is in a circular orbit, each observation would mark points on an ellipse in the  $P$ - $\dot{P}$  plane

(Freire et al. 2001). With three observations and a good determination of the spin and orbital period, we can, in principal, uniquely constrain the equation of this ellipse, which in turn can provide the intrinsic  $P$ ,  $P_b$ , and  $a \sin i/c$ . We attempted to perform this fit to our data using a least squares minimization routine and  $0.01 \text{ lt} - \text{s} \leq a \sin i/c \leq 1000 \text{ lt} - \text{s}$ . We found a best-fit  $a \sin i/c \approx 4.4 \text{ lt} - \text{s}$ , but this solution has poor predictive power (i.e., when we folded our data using this solution, the pulsar was not detected). We were also unable to construct a coherent timing solution in TEMPO2 using this starting orbital solution. We believe that the lack of coverage at multiple orbital phases is limiting our ability to accurately determine  $a \sin i/c$ . It is also possible that NGC 6624F is not in a circular orbit.

## 5. Conclusion

We set out to obtain full timing solutions for nine previously known GC pulsars in M62, NGC 6544, and NGC 6624 (three of which have never been published). Our efforts were successful for six of these pulsars, and a seventh now has a partial solution. We have confirmed the nature of three black widow pulsars (M62E and F, and NGC 6544A). NGC 6544A has  $\dot{P} < 0$ , providing unambiguous evidence that  $\dot{P}$  is dominated by acceleration in the cluster potential, and providing us with a probe of  $\Upsilon_V$  in the cluster core. We find  $\Upsilon_V \gtrsim 0.072$  which, while not very constraining, is consistent with small amounts of low-luminosity matter such as massive black holes or other stellar remnants. We are also able to confirm that NGC 6624C belongs to a rare class of non-recycled GC pulsars similar to the slow pulsars found in the Galactic disk.

The highlight of our work is unquestionably NGC 6544B. This binary MSP is in a highly eccentric orbit and exhibits clear orbital precession and Shapiro delay. Under the well justified assumption that this is due almost entirely to GR, we are able to obtain a most-probable total system mass of  $2.57190(73) M_\odot$ , companion mass of  $1.2064(20) M_\odot$ , and pulsar mass of  $1.3655(21) M_\odot$ . This is the highest mass companion known to orbit a fully recycled MSP, and raises the possibility that NGC 6544B is part of either double neutron star system, which could form via exchange interactions in the GC.

We are deeply grateful to Andrea Possenti and Alessandro Corongiu for providing us with data collected by the Parkes Telescope that was used to check for phase connection in our solutions for M62D, E, and F. We would also like to thank an anonymous referee for helpful comments. R. Lynch acknowledges support from the GBT Student Support program and the National Science Foundation grant AST-0907967 during the course of this work. The National Radio Astronomy Observatory is a facility of the National Science Foundation operated under cooperative agreement by Associated Universities, Inc.

## REFERENCES

- Alpar, M. A., Cheng, A. F., Ruderman, M. A., & Shaham, J. 1982, *Nature*, 300, 728
- Anderson, S. B., Gorham, P. W., Kulkarni, S. R., Prince, T. A., & Wolszczan, A. 1990, *Nature*, 346, 42
- Biggs, J. D., Bailes, M., Lyne, A. G., Goss, W. M., & Fruchter, A. S. 1994, *MNRAS*, 267, 125
- Boyles, J., Lorimer, D. R., Turk, P. J., Mnatsakanov, R., Lynch, R. S., Ransom, S. M., Freire, P. C., & Belczynski, K. 2011, *ArXiv e-prints*
- Camilo, F. & Rasio, F. A. 2005, in *Astronomical Society of the Pacific Conference Series*, Vol. 328, *Binary Radio Pulsars*, ed. F. A. Rasio & I. H. Stairs, 147
- Carretta, E., Gratton, R. G., Clementini, G., & Fusi Pecci, F. 2000, *ApJ*, 533, 215
- Chandler, A. M. 2003, PhD thesis, California Institute Of Technology
- Cocozza, G., Ferraro, F. R., Possenti, A., Beccari, G., Lanzoni, B., Ransom, S., Rood, R. T., & D’Amico, N. 2008, *ApJ*, 679, L105
- D’Amico, N., Lyne, A. G., Manchester, R. N., Possenti, A., & Camilo, F. 2001a, *ApJ*, 548, L171
- D’Amico, N., Possenti, A., Fici, L., Manchester, R. N., Lyne, A. G., Camilo, F., & Sarkissian, J. 2002, *ApJ*, 570, L89
- D’Amico, N., Possenti, A., Manchester, R. N., Sarkissian, J., Lyne, A. G., & Camilo, F. 2001b, *ApJ*, 561, L89
- Dessart, L., Burrows, A., Ott, C. D., Livne, E., Yoon, S., & Langer, N. 2006, *ApJ*, 644, 1063
- DuPlain, R., Ransom, S., Demorest, P., Brandt, P., Ford, J., & Shelton, A. L. 2008, in *Society of Photo-Optical Instrumentation Engineers (SPIE) Conference Series*, Vol. 7019, *Society of Photo-Optical Instrumentation Engineers (SPIE) Conference Series*, 70191D–70191D–10
- Edwards, R. T., Hobbs, G. B., & Manchester, R. N. 2006, *MNRAS*, 372, 1549
- Freire, P. C., Kramer, M., & Lyne, A. G. 2001, *MNRAS*, 322, 885
- Freire, P. C. C. 2005, in *Astronomical Society of the Pacific Conference Series*, Vol. 328, *Binary Radio Pulsars*, ed. F. A. Rasio & I. H. Stairs, 405



- Freire, P. C. C., Bassa, C. G., Wex, N., Stairs, I. H., Champion, D. J., Ransom, S. M., Lazarus, P., Kaspi, V. M., Hessels, J. W. T., Kramer, M., Cordes, J. M., Verbiest, J. P. W., Podsiadlowski, P., Nice, D. J., Deneva, J. S., Lorimer, D. R., Stappers, B. W., McLaughlin, M. A., & Camilo, F. 2011, *MNRAS*, 412, 2763
- Freire, P. C. C., Hessels, J. W. T., Nice, D. J., Ransom, S. M., Lorimer, D. R., & Stairs, I. H. 2005, *ApJ*, 621, 959
- Freire, P. C. C., Ransom, S. M., Bégin, S., Stairs, I. H., Hessels, J. W. T., Frey, L. H., & Camilo, F. 2008, *ApJ*, 675, 670
- Freire, P. C. C., Ransom, S. M., & Gupta, Y. 2007, *ApJ*, 662, 1177
- Freire, P. C. C. & Wex, N. 2010, *MNRAS*, 409, 199
- Harris, W. E. 1996, *AJ*, 112, 1487 (arXiv:1012.3224)
- Haslam, C. G. T., Salter, C. J., Stoffel, H., & Wilson, W. E. 1982, *A&AS*, 47, 1
- Hessels, J. W. T., Ransom, S. M., Stairs, I. H., Freire, P. C. C., Kaspi, V. M., & Camilo, F. 2006, *Science*, 311, 1901
- Hotan, A. W., van Straten, W., & Manchester, R. N. 2004, *PASA*, 21, 302
- Jacoby, B. A., Cameron, P. B., Jenet, F. A., Anderson, S. B., Murty, R. N., & Kulkarni, S. R. 2006, *ApJ*, 644, L113
- Kaplan, D. L., Escoffier, R. P., Lacasse, R. J., O’Neil, K., Ford, J. M., Ransom, S. M., Anderson, S. B., Cordes, J. M., Lazio, T. J. W., & Kulkarni, S. R. 2005, *PASP*, 117, 643
- King, A. R. 1988, *QJRAS*, 29, 1
- King, A. R., Beer, M. E., Rolfe, D. J., Schenker, K., & Skipp, J. M. 2005, *MNRAS*, 358, 1501
- Kitaura, F. S., Janka, H., & Hillebrandt, W. 2006, *A&A*, 450, 345
- Lange, C., Camilo, F., Wex, N., Kramer, M., Backer, D. C., Lyne, A. G., & Doroshenko, O. 2001, *MNRAS*, 326, 274
- Lynch, R. S., Lorimer, D. D., Ransom, S. M., & Boyles, J. in prep., *ApJ*
- Lyne, A. G., Manchester, R. N., & D’Amico, N. 1996, *ApJ*, 460, L41

- Martin, R. G., Tout, C. A., & Pringle, J. E. 2009, *MNRAS*, 397, 1563
- Nice, D. J., Arzoumanian, Z., & Thorsett, S. E. 2000, in *Astronomical Society of the Pacific Conference Series*, Vol. 202, IAU Colloq. 177: Pulsar Astronomy - 2000 and Beyond, ed. M. Kramer, N. Wex, & R. Wielebinski, 67
- Nomoto, K. 1984, *ApJ*, 277, 791
- . 1987, *ApJ*, 322, 206
- Pfahl, E., Rappaport, S., Podsiadlowski, P., & Spruit, H. 2002, *ApJ*, 574, 364
- Phinney, E. S. 1992, *Royal Society of London Philosophical Transactions Series A*, 341, 39
- Phinney, E. S. 1993, in *Astronomical Society of the Pacific Conference Series*, Vol. 50, *Structure and Dynamics of Globular Clusters*, ed. S. G. Djorgovski & G. Meylan, 141
- Possenti, A., D’Amico, N., Manchester, R. N., Camilo, F., Lyne, A. G., Sarkissian, J., & Corongiu, A. 2003, *ApJ*, 599, 475
- Ransom, S. M. 2008, in *American Institute of Physics Conference Series*, Vol. 983, *40 Years of Pulsars: Millisecond Pulsars, Magnetars and More*, ed. C. Bassa, Z. Wang, A. Cumming, & V. M. Kaspi, 415–423
- Ransom, S. M., Greenhill, L. J., Herrnstein, J. R., Manchester, R. N., Camilo, F., Eikenberry, S. S., & Lyne, A. G. 2001, *ApJ*, 546, L25
- Ransom, S. M., Hessels, J. W. T., Stairs, I. H., Freire, P. C. C., Camilo, F., Kaspi, V. M., & Kaplan, D. L. 2005, *Science*, 307, 892
- Shklovskii, I. S. 1970, *Soviet Ast.*, 13, 562
- Splaver, E. M., Nice, D. J., Arzoumanian, Z., Camilo, F., Lyne, A. G., & Stairs, I. H. 2002, *ApJ*, 581, 509
- Taylor, J. H. & Weisberg, J. M. 1989, *ApJ*, 345, 434
- Valenti, E., Origlia, L., & Rich, R. M. 2011, *MNRAS*, 560
- Verbiest, J. P. W., Bailes, M., van Straten, W., Hobbs, G. B., Edwards, R. T., Manchester, R. N., Bhat, N. D. R., Sarkissian, J. M., Jacoby, B. A., & Kulkarni, S. R. 2008, *ApJ*, 679, 675
- Webbink, R. F. 1985, in *IAU Symposium*, Vol. 113, *Dynamics of Star Clusters*, ed. J. Goodman & P. Hut, 541–577

Wong, T., Willems, B., & Kalogera, V. 2010, ApJ, 721, 1689

Table 1. Summary of Pulsars in this Study

Pulsar	Previous Full Timing Solution?	New Full Timing Solution?	Reference
M62			
J1701–3006A	Yes	Yes	A,B
J1701–3006B	Yes	Yes	B
J1701–3006C	Yes	Yes	B
J1701–3006D	No	Yes	C
J1701–3006E	No	Yes	C
J1701–3006F	No	Yes	C
NGC 6544			
J1807–2459A	No	Yes	A,D
J1807–2500B	No	Yes	C
NGC 6624			
J1823–3021A	Yes	Yes	E
J1823–3021B	Yes	Yes	E
J1823–3021C	No	Yes	C
J1823–3021D	No	Yes	Unpublished
J1823–3021E	No	No	Unpublished
J1823–3021F	No	No	Unpublished

References. — A—D’Amico et al. (2001a); B—Possenti et al. (2003);  
 C—Chandler (2003); D—Ransom et al. (2001); E—Biggs et al. (1994)

Table 2. Globular Cluster Properties

ID	$\ell^a$ (deg)	$b^b$ (deg)	$D^c$ (kpc)	$r_c^d$ (arcmin)	$\mu_V^e$ (mag arcsec <sup>-2</sup> )	$\sigma_v^f$ (km s <sup>-1</sup> )
M62	353.57	7.32	6.7	0.22	15.10	13.3
NGC 6544	5.84	-2.20	3.0	0.05	16.31	5.89
NGC 6624	2.78	-7.91	7.8	0.06	15.32	6.0

<sup>a</sup>Galactic longitude

<sup>b</sup>Galactic latitude

<sup>c</sup>Distance

<sup>d</sup>Core radius

<sup>e</sup>Central V-band surface brightness

<sup>f</sup>Central velocity dispersion

Note. — All properties are taken from Harris (1996, 2010 edition), except for  $\sigma_v$  in M62 and NGC 6544 (Webbink 1985), and NGC 6624 (Valenti et al. 2011).

Table 3. Parameters of the Previously Timed Pulsars in M62

Parameter	J1701–3006A	J1701–3006B	J1701–3006C
Timing Parameters			
Right Ascension (J2000) .....	17:01:12.50942(49)	17:01:12.6677(10)	17:01:12.86592(35)
Declination (J2000) .....	–30:06:30.173(36)	–30:06:49.044(76)	–30:06:59.415(21)
Spin Period (s) .....	0.0052415662037958(29)	0.0035938521270515(34)	0.0076128487111379(68)
Period Derivative ( $s s^{-1}$ ) .....	$-1.301(15) \times 10^{-19}$	$-3.483(20) \times 10^{-19}$	$-6.413(10) \times 10^{-20}$
Dispersion Measure ( $pc cm^{-3}$ ) .....	114.9654(84)	115.21(38)	114.5619(69)
Reference Epoch (MJD) .....	55038.0	55038.0	55038.0
Span of Timing Data (MJD) .....	53150–55200	53315–55200	53315–55200
Number of TOAs .....	80	81	74
RMS Timing Residual ( $\mu s$ ) .....	6.4	11.3	15.1
Error Factor .....	1.6	1.5	1.2
Binary Parameters			
Orbital Period (days) .....	3.8059483732(58)	0.14454541718(58)	0.21500007119(51)
Projected Semi-major Axis (lt-s) .....	3.4837397(19)	0.2527565(28)	0.1928816(33)
Epoch of Periastron Passage (MJD) .....	55040.03822060(36)	55038.62576448(54)	55037.92664751(74)
Orbital Eccentricity .....	$< 1.8 \times 10^{-6}$	$< 4.5 \times 10^{-5}$	$< 7.9 \times 10^{-5}$
Longitude of Periastron Passage (deg) ...	...	...	...
Rate of Change of Orbital Period ( $10^{-12}$ )	...	$-5.12(62) \times 10^{-12}$	...
Derived Parameters			
Mass Function ( $M_{\odot}$ ) .....	0.0031339643(51)	0.000829814(27)	0.0001666778(87)
Minimum Companion Mass ( $M_{\odot}$ ) .....	0.2	0.12	0.071
Offset from Cluster Center (core radii) ...	1.50	0.138	0.773
Intrinsic Spin-down ( $s s^{-1}$ ) .....	$\leq 3.13 \times 10^{-19}$	$\leq 4.4 \times 10^{-20}$	$\leq 3.78 \times 10^{-19}$
Surface Magnetic Field ( $10^9$ Gauss) .....	$\leq 1.3$	$\leq 0.4$	$\leq 1.7$
Spin-down Luminosity ( $10^{34}$ erg $s^{-1}$ ) .....	$\leq 8.6$	$\leq 3.7$	$\leq 3.4$
Characteristic Age ( $10^9$ yr) .....	$\geq 0.27$	$\geq 1.3$	$\geq 0.32$
Mean 2 GHz Flux Density ( $\mu Jy$ ) .....	117	78	72

Note. — Numbers in parentheses represent  $1\text{-}\sigma$  uncertainties in the last digits as determined by `TEMP02`, scaled such that the  $\chi^2_{\text{red}} = 1$ . All timing solutions use the DE405 Solar System Ephemeris and the TT(BIPM2011) time standard. All values are reported in Barycentric Dynamical Time (TDB) units. Mean flux density estimates have a typical 10%–20% relative error. Minimum companion masses were calculated assuming a  $1.4 M_{\odot}$  pulsar.

Table 4. Parameters of the Newly Timed Pulsars in M62

Parameter	J1701–3006D	J1701–3006E	J1701–3006F
Timing Parameters			
Right Ascension (J2000) .....	17:01:13.5631(15)	17:01:13.2734(17)	17:01:12.8222(15)
Declination (J2000) .....	–30:06:42.559(79)	–30:06:46.89(11)	–30:06:51.82(10)
Spin Period (s) .....	0.0034177704450548(17)	0.0032337373331158(65)	0.0022947270806719(29)
Period Derivative ( $\text{s s}^{-1}$ ) .....	$1.257(24) \times 10^{-19}$	$3.103(27) \times 10^{-19}$	$2.221(18) \times 10^{-19}$
Dispersion Measure ( $\text{pc cm}^{-3}$ ) .....	114.224(11)	113.792(22)	113.291(34)
Reference Epoch (MJD) .....	55038.0	55038.0	55038.0
Span of Timing Data (MJD) .....	54876–55200	54876–55200	54876–55200
Number of TOAs .....	45	40	47
RMS Timing Residual ( $\mu\text{s}$ ) .....	6.5	13.1	19.5
Error Factor .....	1.1	1.4	1.3
Binary Parameters			
Orbital Period (days) .....	1.1179034034(82)	0.1584774951(56)	0.2054870422(72)
Projected Semi-major Axis (lt-s) .....	0.9880185(50)	0.0701589(55)	0.0573400(52)
Epoch of Periastron Passage (MJD) ..	55037.88706413(93) <sup>a</sup>	55037.9364630(50)	55038.0892403(49)
Orbital Eccentricity .....	0.0004122(67)	$< 1.9 \times 10^{-4}$	$< 3.4 \times 10^{-4}$
Longitude of Periastron Passage (deg)	101.6(1.3)	...	...
Derived Parameters			
Mass Function ( $M_{\odot}$ ) .....	0.000828647(13)	$1.47637(35) \times 10^{-5}$	$4.7939(13) \times 10^{-6}$
Minimum Companion Mass ( $M_{\odot}$ ) ....	0.12	0.031	0.021
Offset from Cluster Center (core radii)	0.912	0.503	0.185
Intrinsic Spin-down ( $\text{s s}^{-1}$ ) .....	$\leq 3.4 \times 10^{-19}$	$\leq 5.56 \times 10^{-19}$	$\leq 4.14 \times 10^{-19}$
Surface Magnetic Field ( $10^9$ Gauss) ..	$\leq 1.1$	$\leq 1.4$	$\leq 0.99$
Spin-down Luminosity ( $10^{34}$ erg $\text{s}^{-1}$ ) .	$\leq 34$	$\leq 65$	$\leq 140$
Characteristic Age ( $10^9$ yr) .....	$\geq 0.16$	$\geq 0.092$	$\geq 0.088$
Mean 2 GHz Flux Density ( $\mu\text{Jy}$ ) .....	69	39	52



<sup>a</sup>For M62D we give the epoch of the ascending node ( $T_{asc}$ ), which is more precisely measured in the ELL1 timing model.

Note. — See the notes to Table 3 for more details on these timing solutions.

Table 5. Parameters of NGC 6544A

Parameter	J1807–2459A
Timing Parameters	
Right Ascension (J2000) .....	18:07:20.355604(16)
Declination (J2000) .....	–24:59:52.9015(65)
Spin Period (s) .....	0.003059448798020229(30)
Period Derivative (s s <sup>–1</sup> ) .....	–4.3352(26) × 10 <sup>–21</sup>
Dispersion Measure (pc cm <sup>–3</sup> ) .....	134.00401(58)
Reference Epoch (MJD) .....	55243.0
Span of Timing Data (MJD) .....	53315–55760
Number of TOAs .....	296
RMS Timing Residual (μs) .....	1.4
Error Factor .....	1.4
Binary Parameters	
Orbital Period (days) .....	0.071091483516(29)
Projected Semi-major Axis (lt-s) .....	0.01222393(12)
Epoch of Periastron Passage (MJD) .....	55242.99436660(24)
Orbital Eccentricity .....	< 1.1 × 10 <sup>–4</sup>
Longitude of Periastron Passage (deg) ...	...
Rate of Change of Orbital Period (10 <sup>–12</sup> )	–1.142(62) × 10 <sup>–12</sup>
Derived Parameters	
Mass Function (M <sub>⊙</sub> ) .....	3.88043(11) × 10 <sup>–7</sup>
Minimum Companion Mass (M <sub>⊙</sub> ) .....	0.0092
Offset from Cluster Center (core radii) ...	1.31
Intrinsic Spin-down (s s <sup>–1</sup> ) .....	≤ 2.58 × 10 <sup>–19</sup>
Surface Magnetic Field (10 <sup>9</sup> Gauss) .....	≤ 0.9
Spin-down Luminosity (10 <sup>34</sup> erg s <sup>–1</sup> ) .....	≤ 36
Characteristic Age (10 <sup>9</sup> yr) .....	≥ 0.19
Mean 2 GHz Flux Density (μJy) .....	605
Rotation Measure (rad m <sup>–2</sup> ) .....	160.4(6)

Note. — See the notes to Table 3 for more details on this timing solution.

Table 6. Parameters of NGC 6544B using DDGR Model

Parameter	J1807–2500B
Timing Parameters	
Right Ascension (J2000) .....	18:07:20.871209(53)
Declination (J2000) .....	–25:00:1.915(17)
Spin Period (s) .....	0.00418617720284089(25)
Period Derivative ( $\text{s s}^{-1}$ ) .....	$8.23245(18) \times 10^{-20}$
Dispersion Measure ( $\text{pc cm}^{-3}$ ) .....	137.1535(20)
Reference Epoch (MJD) .....	54881.352079
Span of Timing Data (MJD) .....	53315–55760
Number of TOAs .....	278
RMS Timing Residual ( $\mu\text{s}$ ) .....	5.4
Error Factor .....	1.0
Binary Parameters	
Orbital Period (days) .....	9.9566681588(27)
Projected Semi-major Axis (lt-s) .....	28.920391(44)
Epoch of Periastron Passage (MJD) .....	54881.34735776(22)
Orbital Eccentricity .....	0.747033198(40)
Longitude of Periastron Passage (deg) ...	11.334600(18)
Total System Mass ( $M_{\odot}$ ) .....	2.57190(73)
Companion Mass ( $M_{\odot}$ ) .....	1.2064(20)
Derived Parameters	
Pulsar Mass ( $M_{\odot}$ ) .....	1.3655(21)
$\sin i$ .....	0.9956(14)
Mass Function ( $M_{\odot}$ ) .....	0.2619794(12)
Rate of Change of Orbital Period ( $10^{-12}$ )	–0.027921(62)
Rate of Periastron Advance ( $\text{deg yr}^{-1}$ ) ...	0.0183389(35)
Gravitational Redshift (s) .....	0.014418(40)
Offset from Cluster Center (core radii) ...	4.05
Intrinsic Spin-down ( $\text{s s}^{-1}$ ) .....	$\leq 2.25 \times 10^{-19}$
Surface Magnetic Field ( $10^9$ Gauss) .....	$\leq 0.98$
Spin-down Luminosity ( $10^{34}$ erg $\text{s}^{-1}$ ) ....	$\leq 12.0$
Characteristic Age ( $10^9$ yr) .....	$\geq 0.29$
Mean 2 GHz Flux Density ( $\mu\text{Jy}$ ) .....	88
Rotation Measure ( $\text{rad m}^{-2}$ ) .....	157(1)

Note. — In the DDGR model,  $M_{\text{tot}}$  and  $M_c$  are the only free PK parameters. See the notes to Table 3 for more details on this timing solution.

Table 7. Parameters of the Pulsars in NGC 6624

Parameter	J1823–3021A	J1823–3021B	J1823–3021C	J1823–3021D
Timing Parameters				
Right Ascension (J2000) .....	18:23:40.48701(36)	18:23:41.5455(23)	18:23:41.1516(36)	18:23:40.5312(71)
Declination (J2000) .....	–30:21:40.127(44)	–30:21:40.94(47)	–30:21:38.45(80)	–30:21:43.66(35)
Spin Period (s) .....	0.0054400041632727(31)	0.3785964921974(27)	0.4059359629899(53)	0.003020060260978(59)
Period Derivative ( $\text{s s}^{-1}$ ) .....	$3.3750(20) \times 10^{-18}$	$2.99(14) \times 10^{-17}$	$2.240(25) \times 10^{-16}$	...
Dispersion Measure ( $\text{pc cm}^{-3}$ ) .....	86.8797(56)	87.01(10)	86.88(24)	86.8(1.1)
Reference Epoch (MJD) .....	55049.0	55049.0	55049.0	55050.0
Span of Timing Data (MJD) .....	54898–55200	54898–55200	54898–55200	54898–55200
Number of TOAs .....	33	33	31	10
RMS Timing Residual ( $\mu\text{s}$ ) .....	4.6	55.8	104.9	90.0
Error Factor .....	1.1	1.0	1.1	3.9
Derived Parameters				
Offset from Cluster Center (core radii)	0.115	3.74	2.24	2.33
Intrinsic Spin-down ( $\text{s s}^{-1}$ ) .....	$\leq 3.64 \times 10^{-16}$	$\leq 3.45 \times 10^{-17}$	$\leq 2.33 \times 10^{-16}$	...
Surface Magnetic Field ( $10^9$ Gauss) ..	$\leq 45$	$\leq 120$	$\leq 310$	...
Spin-down Luminosity ( $10^{34}$ erg $\text{s}^{-1}$ ) .	$\leq 8900$	$\leq 0.0025$	$\leq 0.014$	...
Characteristic Age ( $10^9$ yr) .....	$\geq 0.00024$	$\geq 0.17$	$\geq 0.028$	...
Mean 2 GHz Flux Density ( $\mu\text{Jy}$ ) .....	79	76	37	29

Note. — See the notes to Table 3 for more details on these timing solutions.

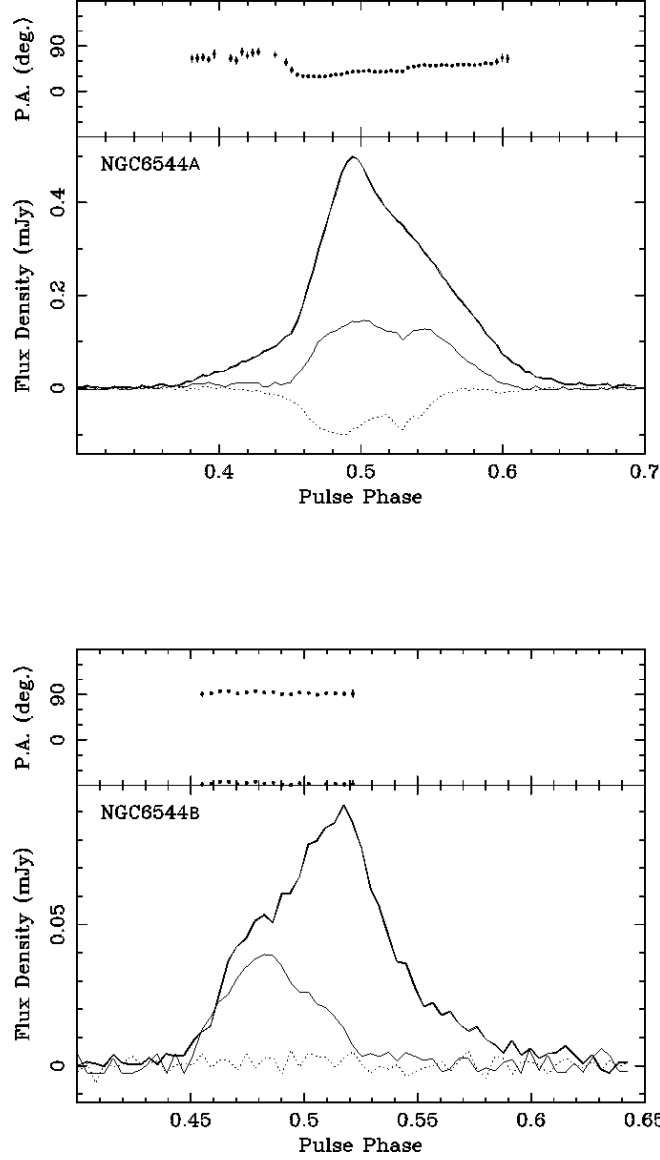


Fig. 1.— Calibrated pulse profiles for NGC 6544A and B showing the integrated pulse profile (top solid lines) and the fraction of linear (second solid line) and circular (dotted line) polarization. The top panels show the polarization angle. The profiles have been rotated by an arbitrary amount. These data are from our Shapiro delay observations for NGC 6544B (see §4.6) and were taken at 1.4 GHz in a coherent de-dispersion mode. The sampling time was  $10.24 \mu\text{s}$  (0.3% and 0.2% of pulse phase for NGC 6544A and B, respectively).

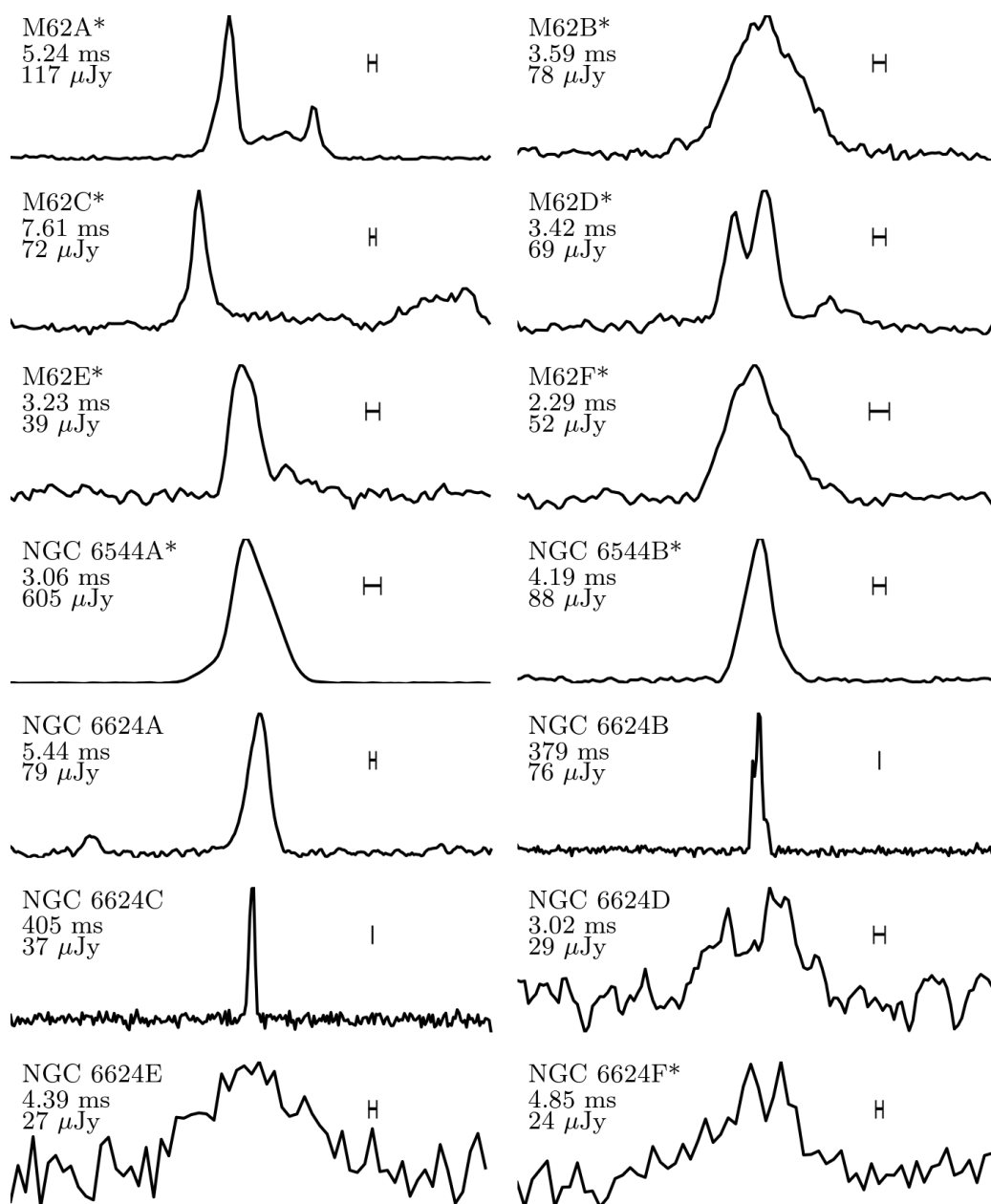


Fig. 2.— Average 2 GHz pulse profiles for all pulsars in these clusters. Binary pulsars are denoted by an asterisk. These profiles formed the basis of the standards used in our timing analysis, and were created by summing all the detections of a given pulsar. In the case of the pulsars in NGC 6624, only data de-dispersed at the correct DM was used for making these plots (see text for more details). The bars indicate the contribution of dispersive smearing to the profile width.

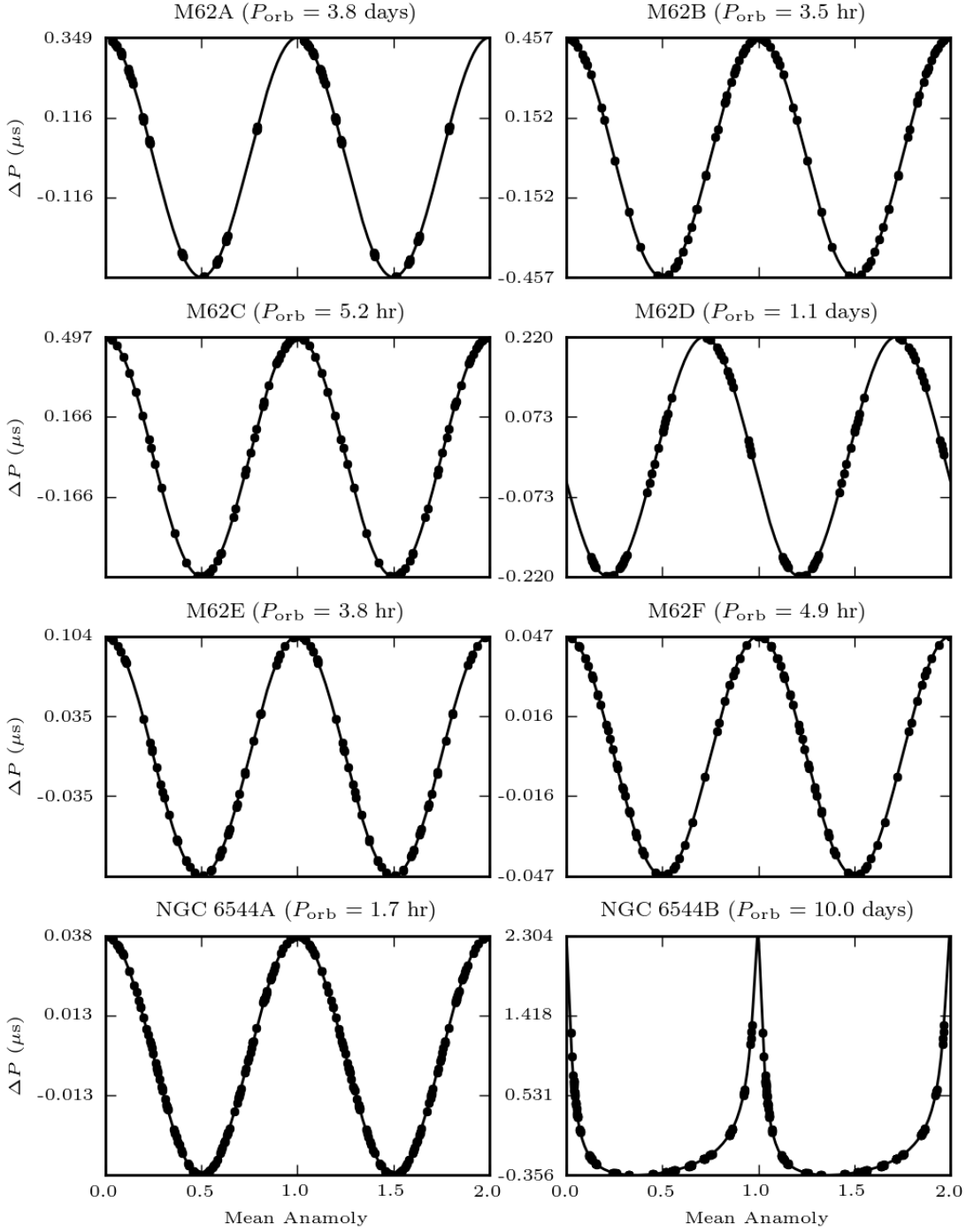


Fig. 3.— The change in observed rotational period due to the Doppler effect as a function of mean anomaly. The circles show the observed periods. For clarity, the data are duplicated from orbital phase 1–2. Note that the high eccentricity of NGC 6544B causes the large deviation from a sinusoidal modulation of the period.

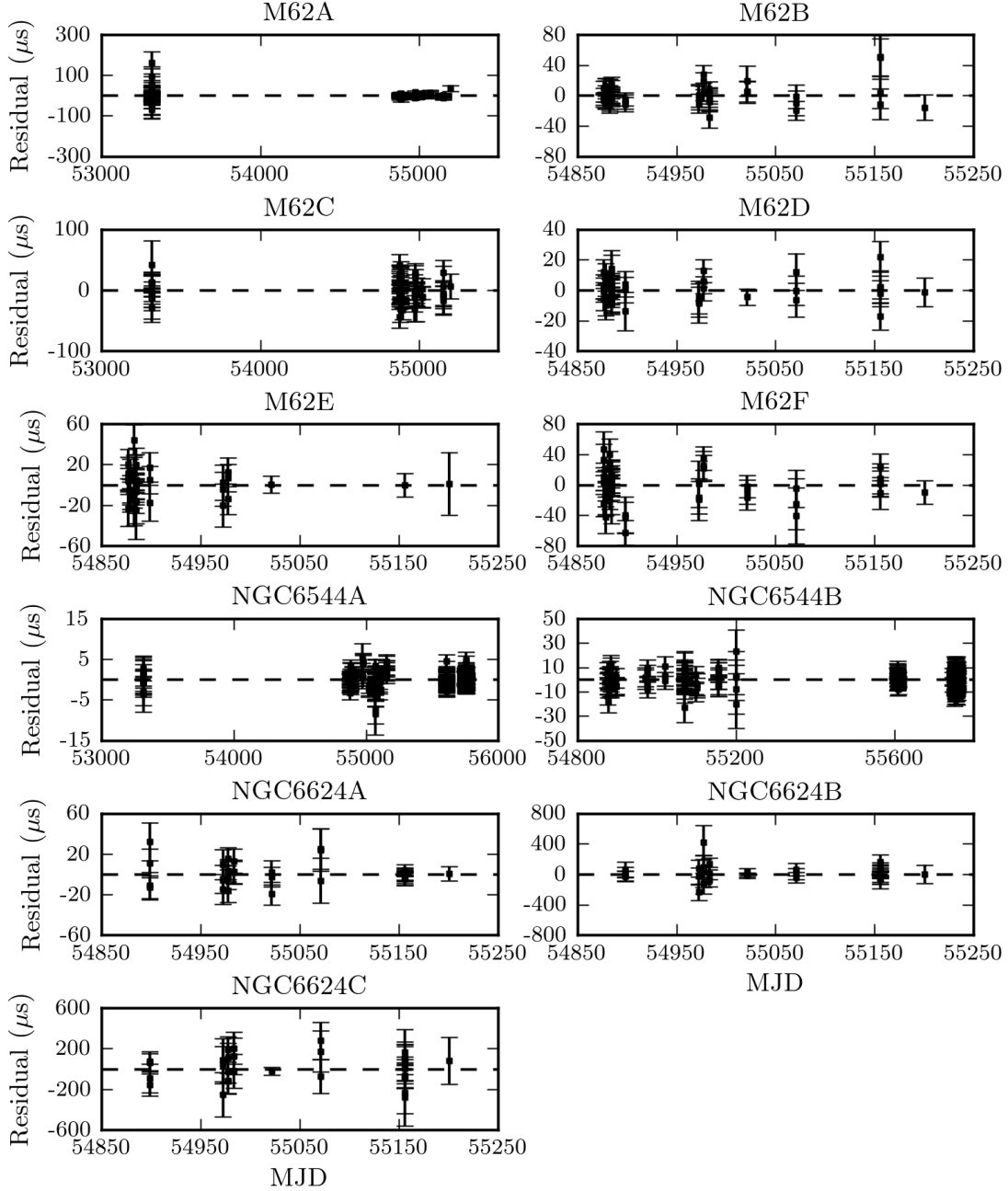


Fig. 4.— Post-fit timing residuals for the pulsars in these clusters. Only unambiguously phase connected TOAs are displayed. The TOAs around MJD 55600 for NGC 6544A and B are from recent Shapiro delay observations of NGC 6544B.



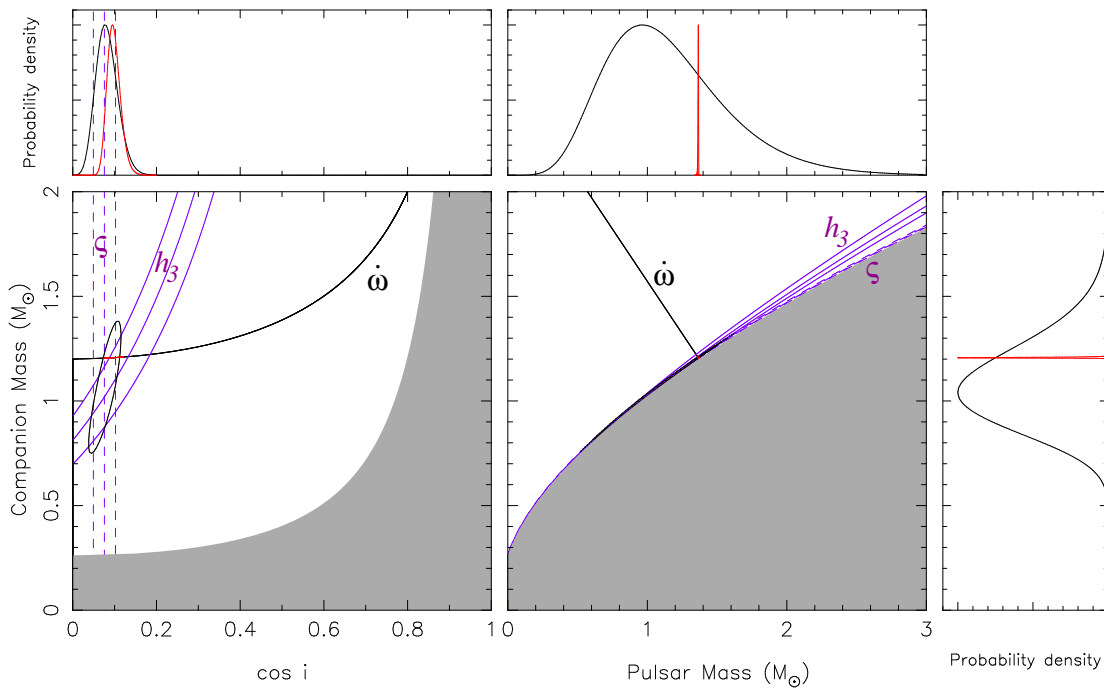


Fig. 5.— Constraints on the inclination angle and masses in NGC 6544B from  $\chi^2$  maps and the DDH timing model. Our measurement of  $\dot{\omega}$  implies a total mass of  $2.57190(73) M_{\odot}$ , indicated by the black lines. The  $1\text{-}\sigma$  uncertainty is so small that it is invisible at this scale. The solid purple lines indicate the constraints from  $h_3$  and the dashed purple lines indicate the constraints from  $\zeta$ . *Left*:  $\cos i$ - $M_c$  plot. The gray region is excluded by the condition  $M_p > 0$ . *Right*:  $M_p$ - $M_c$  plot. The gray region is excluded by the condition  $|\sin i| \leq 1$ . The black contours include 68.3% of the total probability of a 2-D probability distribution function (PDF), calculated from a  $\chi^2$  map that used only the Shapiro delay to constrain the masses. The red contour levels further assume that GR is correct and is the sole cause of  $\dot{\omega}$ . *Top and right marginal plots*: 1-D PDFs for  $\cos i$ ,  $M_p$  and  $M_c$ , obtained by marginalization of both 2-D PDFs. The second PDF (in red) yields median masses of  $M_p^{\text{med}} = 1.3649^{+0.0017}_{-0.0022} M_{\odot}$ , and  $M_c^{\text{med}} = 1.2068^{+0.0022}_{-0.0016} M_{\odot}$ . The probability peaks at  $M_p^{\text{max}} = 1.3654 M_{\odot}$  and  $M_c^{\text{max}} = 1.2063 M_{\odot}$ . These are in excellent agreement with the masses obtained from the DDGR timing solution, given in Table 6.